ELSEVIER

Biophysical Chemistry 124 (2006) 27–34

Biophysical Chemistry

http://www.elsevier.com/locate/biophyschem

Stoichiometry of ATP and metal cofactor interaction with the sarcoplasmic reticulum Ca^{2+}–ATPase: A binding model accounting for radioisotopic and fluorescence results

Débora A. González [a,*], Mariano A. Ostuni [b,c], Jean-Jacques Lacapère [b,c], Guillermo L. Alonso [a]

[a] *Cátedra de Biofísica, Facultad de Odontología, Universidad de Buenos Aires, M.T. De Alvear 2142 (C1122AAH) Buenos Aires, Argentina*
[b] *INSERM, U773, Centre de Recherche Biomédicale Bichat Beaujon CRB3, BP 416, F-75018, Paris, France*
[c] *Université Paris 7 Denis Diderot, site Bichat, BP 416, F-75018, Paris, France*

Received 17 May 2006; accepted 21 May 2006
Available online 19 June 2006

Abstract

Sarcoplasmic reticulum Ca–ATPase belongs to the P-type ATPases family and transports calcium at the expense of ATP hydrolysis. For years, a complex pattern of activity has been observed as a function of ATP and metal cofactor concentrations, leaving the stoichiometry of both metal and ATP in the active site as an open question. In agreement with recent structural studies we present here–using Mn as analogue of Mg–radioisotopic and fluorescence results showing that two metal ions bind to the Ca–ATPase favoring ATP binding. We further show that low ATP concentration favors the binding of these ions, whereas high ATP concentration is inhibitory. We propose a binding model for ATP and metal ions, which permits simulation of our data. Finally, we suggest that (i) the contribution of two metal ions as cofactors of ATP is essential to get maximal activity; (ii) the contribution of two ATP molecules can activate or inhibit the Ca–ATPase depending on metal concentration.

Keywords: Sarcoplasmic reticulum Ca^{2+}–ATPase; ATPase activity; ATP sites; Magnesium sites; Intrinsic fluorescence; ^{54}Mn

1. Introduction

Calcium pumps belonging to the P-type ATPases family maintain intracellular calcium concentrations at a low level. Among them, the SERCA1a from sarcoplasmic reticulum (SR) of rabbit skeletal muscle is one of the most studied. Calcium transport by this SR–Ca^{2+}–ATPase proceeds at the expense of ATP hydrolysis and the reaction cycle can be schematically presented as shown in Scheme 1, where the enzyme can be represented in two main conformational states: E_1 in the presence of calcium and E_2 in its absence.

At neutral pH, and in the absence of ATP or Pi in the incubation media, contaminant calcium is enough to saturate the transport sites, and the enzyme is in the $E_1{\cdot}Ca_2$ form. At acidic pH, protons compete with calcium for the transport sites and the enzyme is predominantly in a protonated form (E_2) [1,2]. $E_1{\cdot}Ca_2$ is phosphorylated by ATP and E_2 by Pi. ATP binds to E_2 without being hydrolyzed until Ca^{2+} is available [3]. Mg^{2+} is the physiological cosubstrate for both ATP and Pi in the forward and reversal reactions, respectively, and probably it remains bound during the enzyme cycle [4–7]. Although enzyme mechanism has been intensively studied, the stoichiometries for ATP and Mg^{2+} interacting with the active site are still open questions. Only one Mg^{2+} would be enough to phosphorylate the enzyme and allow pump operation in the presence of micromolar ATP [8,9]. However, ATP and Mg^{2+}, in addition to be the phosphorylation substrates, exert modulatory effects on several steps of the enzyme cycle. ATP concentrations higher than that required for phosphoenzyme formation accelerate ATP hydrolysis. Two distinct ATP sites, catalytic and regulatory, have been proposed either in a monomeric enzyme unit or in different and interacting units [10–13], although another accepted explanation is that a second ATP binds with lower affinity to the same site after phosphorylation and ADP dissociation [14,15]. Recently, and based on structural studies, considering a second ATP site at a location different from that of the substrate site was presented as an attractive hypothesis [16].

* Corresponding author. Tel./fax: +54 11 4964 1298.
E-mail address: debora@biofis.odon.uba.ar (D.A. González).

0301-4622/$ - see front matter © 2006 Elsevier B.V. All rights reserved.
doi:10.1016/j.bpc.2006.05.025

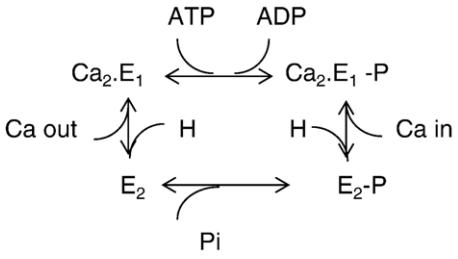

Scheme 1. Schematic reaction cycle of the SR Ca-ATPase.

Furthermore, in addition to being the ATP cosubstrate for phosphorylation, Mg^{2+} is also an activator of E–P hydrolysis [17] and a regulatory Mg site has been proposed based on functional studies [6,18]. High-affinity metal (Me^{2+}) binding to the catalytic site can be studied using [^{54}Mn]Mn, an Mg analogue [4,5,9,19]. In a previous work, we investigated the Mn^{2+} stoichiometry in enzyme phosphorylation with Pi and showed that 2 Mn^{2+}, bound with micromolar and millimolar affinities to the enzyme, are required for maximal phosphorylation [20]. Our finding allows considering the existence of two metallic sites closely interacting with the phosphorylation site. Using Fe^{2+} as ATP cosubstrate, models for two Mg^{2+} binding sites were recently proposed for different P-type pumps [21–23]. Recently, it was reported in structural studies that 2 Mg^{2+} ions participate in phosphoryl transfer from ATP to Asp351 [24].

Here, we present experimental in vitro and in silico results showing the binding of 2 Me^{2+} to the Ca–ATPase as cofactors of ATP and also supporting the hypothesis of 2 different sites for ATP. We studied the Me^{2+} dependence of the ATPase activity throughout an extended range of Mn^{2+} and Mg^{2+} concentrations with both micromolar and millimolar ATP. We took advantage of the acidic pH (5.5) to study the interaction of Mn^{2+} and ATP with the catalytic site, without phosphorylation of the enzyme. We measured the effect of different ATP concentrations on high affinity [^{54}Mn]Mn binding and the effect of micromolar and millimolar Mn concentrations on the intrinsic fluorescence changes associated with ATP binding. We propose a binding model for ATP and Mn^{2+} at equilibrium (i.e., without enzyme turnover), which is compatible with binding and ATPase activity measurements at different ATP and Me^{2+} concentrations.

2. Materials and methods

Sarcoplasmic reticulum vesicles from rabbit skeletal muscles were obtained as described by Champeil et al. [25]. The procedure yields a SR fraction with high Ca-dependent ATPase activity and very low basal ATPase activity (less than 5%) measured in the absence of Ca^{2+} and in the presence of different $MgCl_2$ concentrations. The protein concentration of the membrane suspensions was measured by the method of Lowry et al. [26], using bovine serum albumin as standard.

The ATPase activity was measured at pH 7.2 and 37 °C following Pi liberation. The media contained 50 mM MOPS–Tris, 0.1 M KCl, 20 μM added $CaCl_2$ (or 0.1 mM EGTA–0.1 mM $CaCl_2$, giving 10–20 μM free calcium), and ATP, $MgCl_2$ or $MnCl_2$ as indicated below. When indicated, 0.01 mM Ca ionophore A23187 was included. Reactions were started by addition of 20 μg / ml of SR protein. After 10 s or 1 min incubations, in the presence of 30 μM or 3 mM ATP respectively, the reactions were stopped by addition of cold trichloroacetic acid at 5% final concentration. Pi production was determined with the colorimetric technique of Baginski et al. [27].

The binding of Mn^{2+} was measured using [^{54}Mn]Mn. SR vesicles (0.6–0.8 mg/ml) were incubated for 15 s at 0 °C in 100 mM MES-tris (pH 5.5) and different amounts of [^{54}Mn] $MnCl_2$ and ATP. Measurements at pH 7.2 were made in media with 100 mM Mops–Tris and different amounts of [^{54}Mn] $MnCl_2$ and $MgCl_2$. The media were filtered through Millipore filters (HAWP 0.45 μm average pore), and the radioactivity retained in the filters was measured in a gamma scintillation counter. Data from filters without SR membranes were subtracted.

The intrinsic fluorescence of the Ca–ATPase was correlated to ligand interactions with the protein. The reactions were carried out at 20 °C and pH 5.5. The fluorescence measurements were performed in a Hitachi F-2500 spectrophotometer. The wavelengths were set at 290 nm and 330 nm for excitation and emission, respectively. SR vesicles were suspended at 0.125 mg protein/ml in a 2 ml medium containing 100 mM MES-tris. Changes in fluorescence intensity were corrected for dilution and substrates absorption. The fluorescence variations induced by each ATP concentration were obtained adding at once the ATP needed to reach the desired concentration.

[^{54}Mn]$MnCl_2$ was obtained from New England Nuclear, E.I. Dupont de Nemours, Boston MA. ATP.Na_2 was from Sigma Chem. Co., St Louis, MO. All other reagents were analytical grade.

The fitted curves shown in Fig. 4 (inset) and 5B were computed with a program simulating the binding models depicted below. The equilibrium concentrations of the species were calculated from their initial concentrations and the equilibrium constants deduced from the experimental results.

Equilibrium constants for MgATP and MnATP were calculated from absolute constants [28], taking into account the ATP forms present at pH 5.5 or 7.2.

3. Results

3.1. ATPase activity

Millimolar ATP concentrations, very much higher than those required for phosphoenzyme formation, accelerate ATP hydrolysis. To explain such activating effect, it has been proposed the participation of a second ATP molecule in the enzymatic cycle binding with lower affinity either in a unique ATP site after ADP leaves, or in a different site. Contribution of several cations has also been proposed and in a previous study we showed that two Mn^{2+} (one with micromolar and the other with millimolar affinity) are involved in enzyme phosphorylation by Pi [20]. Therefore, we tested the effect of an extended

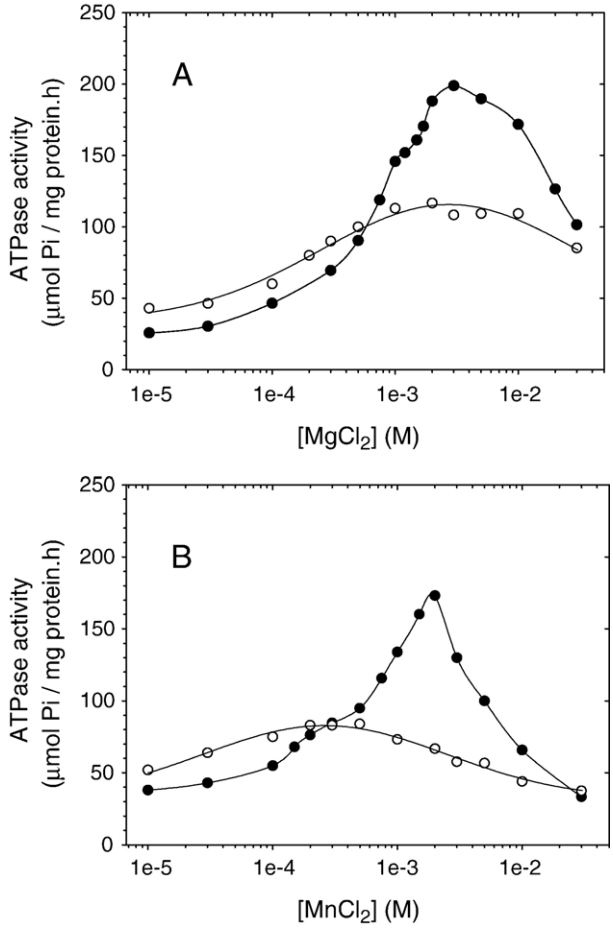

Fig. 1. ATPase activity as a function of $MgCl_2$ (A) and $MnCl_2$ (B) concentrations. Determinations were in the presence of 50 mM Mops–Tris (pH 7.2), 0.1 M KCl, 20 µM $CaCl_2$ and 30 µM (○) or 3 mM (●) ATP, at 37 °C. The curves represent typical experiments.

concentration range of Mn^{2+}, and of the physiological cofactor Mg^{2+}, on ATPase activity. We used low and high ATP concentrations (0.03 and 3 mM) to look for eventually different metal requirements under each condition.

Fig. 1 shows the divalent cation dependence of Pi production at 37 °C and pH 7.2 in the presence of 20 µM added $CaCl_2$. Free calcium concentration cannot be regulated by EGTA because it has higher affinity for Mn^{2+} than for Ca^{2+}. With the low ATP concentration (30 µM) the ATPase activity increased with increasing $MgCl_2$ (Fig. 1A) and $MnCl_2$ (Fig. 1B) concentrations (with K_m around 10^{-4} M and 10^{-5} M, respectively), as previously shown by Ogurusu et al. [9]. Extra activation required both millimolar metal and millimolar ATP. Indeed, with high ATP concentration (3 mM) higher activities were reached with both Mg^{2+} and Mn^{2+}, but a more complex cation dependence of ATPase activity was observed. The rising phases of the curves indicate the participation of more than one metal ion and ATP molecule for maximal enzyme function. The same complex pattern was obtained when the results were plotted against the concentrations of the ATP·Mn or ATP·Mg complexes (not shown). Inhibitory effects of Me and ATP were also observed: On one hand, when metal concentrations were low (below 0.6 mM for Mg and 0.3 mM for Mn), lower activities were observed for the high ATP concentration, showing an inhibitory effect of high ATP. This effect was consistently observed whatever the Ca^{2+} concentration present in the medium (data not shown), which discards that inhibition by high ATP was because of a decreased Ca^{2+} concentration. The results could be due to free Mg^{2+} or Mn^{2+} depletion. On the other hand, the highest metal concentrations inhibited the ATPase activity. This inhibition could be partially explained by previous observations indicating that Mg^{2+} decreases Ca^{2+} affinity for the transport sites [1]. This explanation could also be applied to Mn^{2+}, since it competes with Ca^{2+} for the transport sites and, conversely to Mg, Mn is transported by the Ca–ATPase [29,30].

To further characterize the complex rising phase of ATPase activity upon increasing metal concentration, we repeated them under usual conditions for ATPase activity determinations, i.e., in the presence of calcymicine and EGTA. Fig. 2A shows that the Mg dependence of ATPase activation with 3 mM ATP has similar pattern under both conditions. Fig. 2B shows that the inhibitory effect of 3 mM ATP on ATPase activity compared to lower ATP concentration at 0.3 mM $MgCl_2$ is also observed in the presence of calcymicine and EGTA.

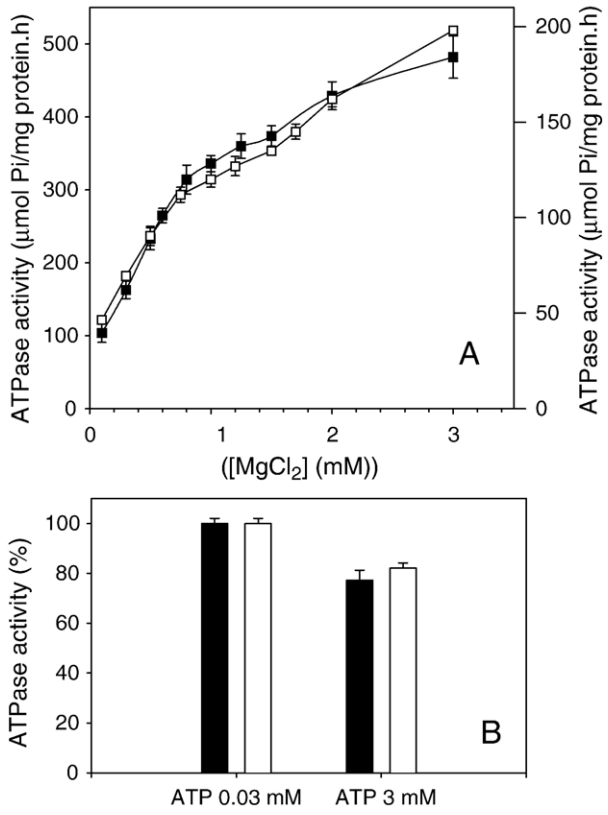

Fig. 2. ATPase activities in the presence of A23187 and EGTA. (A) ATPase activity as a function of $MgCl_2$ with 3 mM ATP, measured as in Fig. 1A (■, right axis) and with the addition of 10 µM calcium ionophore A23187 and replacing 20 µM $CaCl_2$ by 0.1 mM EGTA + 0.1 mM $CaCl_2$ (□, left axis). (B) Inhibitory effect of high [ATP] at low [Me]. Data shown in (A) for 0.3 mM $MgCl_2$ are compared with ATPase activities obtained under the same conditions (without (■) and with (□) A23187) but with 0.03 mM ATP. Shown results are means ± S.E.M. (n = 4).

We suggest that description of ATPase activity variations observed in Figs. 1 and 2 requires the participation of 2 ATP and 2 Me^{2+} with different affinities. To discuss about substrates stoichiometry, the study of Me^{2+} and ATP binding and their eventual reciprocal interactions was necessary.

3.2. Mn and ATP binding

Metal binding to the catalytic site was studied using [^{54}Mn]Mn. We investigated Mn–Mg competition at pH 7.2 for the highest affinity Mn site. Fig. 3 shows [^{54}Mn]Mn binding in the absence or in the presence of increasing $MgCl_2$ concentrations. At $MnCl_2$ concentrations higher than 10 μM and in the absence of Mg, there was an important additional binding probably due to unspecific binding. Therefore, to evaluate only the binding to the highest affinity Mn site, data were fitted with a Hill equation ($n=1$) tending to 5.3 nmol/mg, which was the measured covalent phosphoenzyme amount formed by Pi under optimal experimental conditions in our SR preparation. ATPase affinity for Mn^{2+} ($[Mn]_{1/2} \cong 11$ μM) is close to the K_m for Mn at 30 μM ATP (Fig. 1B). The apparent affinity decreased (i.e., $Mn_{1/2}$ increased) in the presence of Mg^{2+}. The linear relation between $Mn_{1/2}$ and $[Mg^{2+}]$ (Fig. 3, inset) indicates a simple competition for a cation site, and the line's slope allows calculating a K_d around 0.9 mM for Mg^{2+}. The difference between this value and the K_m for Mg at 30 μM ATP (Fig. 1A) could be explained by ATP effect on Mg^{2+} affinity and will be discussed below.

In the absence of calcium in the transport sites, ATP (alone or with its metal cofactor) binds to the catalytic site of the enzyme without being hydrolyzed [3]. At neutral pH, contaminant Ca is enough to saturate the transport sites ($K_d \cong 1$ μM at pH 7.2) leading to full activation of the Ca–ATPase and ATP hydrolysis upon ATP addition. In these conditions, the measurement of ATP binding is impossible. A possibility would be to add calcium chelators, but as mentioned above, EGTA binds Mn strongly and cannot be used to measure Mn binding. On the contrary, contaminant Ca^{2+} (<10 μM) does not saturate the

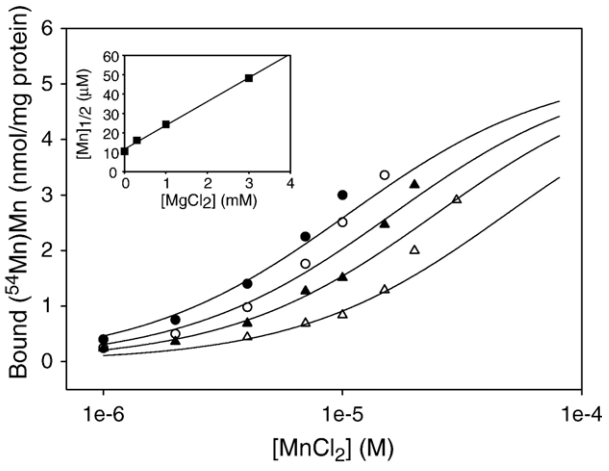

Fig. 3. Mg effect on [^{54}Mn]Mn binding at pH 7.2 The binding of [^{54}Mn]Mn was measured in the presence of 0 (●), 0.3 (○), 1 (▲) and 3 (△) mM $MgCl_2$. Data were fitted with a sigmoid function tending to 5.3 nmol/mg. $Mn_{1/2}$ values were obtained from the curves, and represented as a function of $[Mg^{2+}]$ (inset).

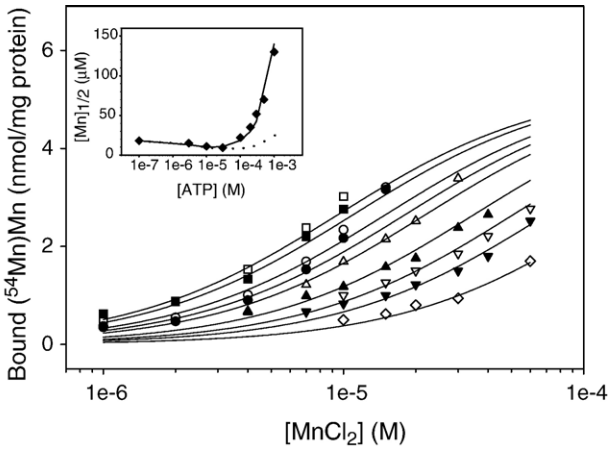

Fig. 4. ATP effect on [^{54}Mn]Mn binding at pH 5.5. The binding of [^{54}Mn]Mn was measured in the presence of 0 (●), 3 (○), 10 (■), 30 (□), 100 (△), 200 (▲), 300 (▽), 500 (▼) and 1000 (◇) μM ATP. Data were fitted with a sigmoid function tending to 5.3 nmol/mg. The inset shows ATP dependence of $[Mn]_{1/2}$ values obtained from curves in the main figure. Lines were obtained by numerical simulation of Models 1 (...) and 3 (−).

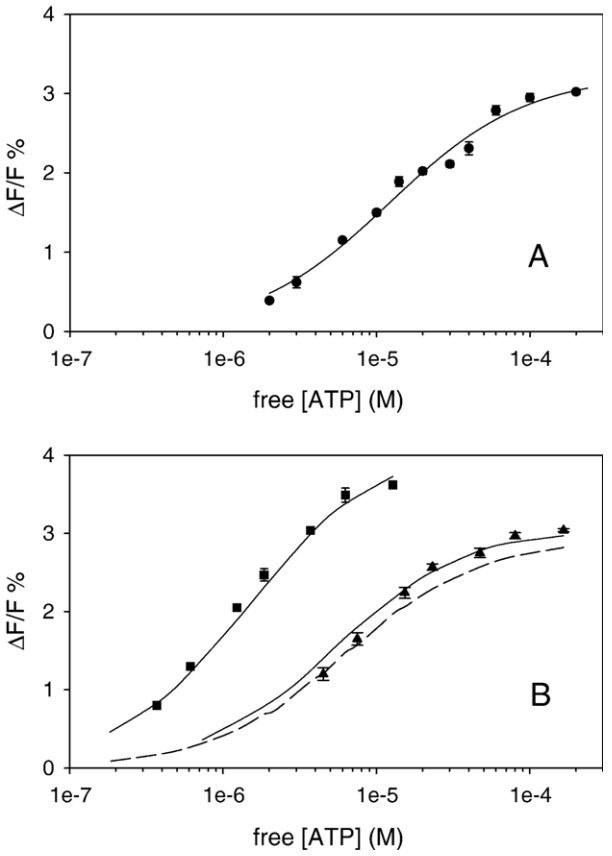

Fig. 5. Effect of Mn on ATP-dependent intrinsic fluorescence changes. (A) Intrinsic fluorescence changes induced by ATP at pH 5.5 in the presence of 2 mM EDTA. Data were fitted with a sigmoid function tending to 3.2%. (B) Intrinsic fluorescence changes induced by ATP at pH 5.5 in the presence of 0.1 mM (▲) and 5 mM (■) $MnCl_2$. Dashed line was obtained by simulation of Model 1 and applies to both [Mn]. Full lines simulate ATP induced fluorescence increase in the presence of 0.1 and 5 mM $MnCl_2$, according to Model 2. Results are means ± S.E.M. ($n \geq 5$).

transport sites at acidic pH ($K_d \cong 50$ μM at pH 5.5) [20] and then the binding of the substrates to E_2 can be studied in the absence of calcium chelators. As a control, we found that while addition of 2 mM EDTA to SR vesicles at pH 7.2 induced a 6–7% decrease in intrinsic fluorescence (due to E_1Ca_2 to E_2 transconformation [31]), the decrease was only 0.2% at pH 5.5 because the enzyme was predominantly in E_2 form prior to EDTA addition. The binding experiments of Mn^{2+} and ATP were carried out at pH 5.5. [^{54}Mn]Mn binding was measured at 2 °C to further minimize the possibility of enzyme cycling.

In a previous work we measured high affinity [^{54}Mn]Mn binding to E_2 at pH 5.5 and assigned it to one of the two Mn^{2+} involved in enzyme phosphorylation with Pi [20]. Now, we studied the effect of ATP on this high affinity Mn^{2+} binding (Fig. 4). Data were also fitted with a sigmoid function tending to 5.3 nmol/mg. Fig. 4 shows that in the absence of ATP, K_d for the highest affinity Mn^{2+} site was ≅18 μM, something higher than K_d=11 μM observed at pH 7.2. ATP up to 30 μM increased Mn affinity but higher ATP concentrations strongly inhibited the cation binding, showing a dual ATP effect (inset Fig. 4 shows changes of $Mn_{1/2}$ as a function of ATP concentrations). These results and those about ATP binding presented below were analyzed together to look for a compatible binding model.

ATP binding can be measured either with radioisotopic or fluorescence techniques. Due to the poor resolution of the radioisotopic technique at high [ATP], the measurement of the changes in the intrinsic fluorescence of the Ca–ATPase is used as an index of ATP binding [3]. Fig. 5A shows ATP-dependent fluorescence increase as a function of ATP concentration (up to 0.2 mM), at pH 5.5 and in the absence of Mn. Fluorescence increased up to 3.2% with apparent affinity of 12 μM. Fig. 5B shows Mn effect on ATP-dependent fluorescence changes. Fluorescence data show that true affinity for ATP was changed in the presence of Mn: K_d was around 5 μM and 1 μM with 0.1 mM and 5 mM $MnCl_2$, respectively. According to ^{54}Mn binding results (Fig. 4), in the presence 0.1 mM Mn^{2+} and 0.2 mM ATP (maximal [ATP] used in fluorescence experiments) almost 100% of the ATPase molecules has 1 Mn^{2+} bound. Fig. 5B also shows that with 0.1 mM Mn^{2+} the fluorescence increased up to 3% but with 5 mM Mn^{2+} the ATP-dependent fluorescence increment was higher (close to 4%) . This suggests the appearance of a different enzymatic conformation in the presence of enough ATP and high Mn concentration. Taking into account the participation of 2 Mn^{2+} in enzyme phosphorylation with Pi with micromolar and millimolar affinities [20] and the biphasic increment of the ATPase activity as a function of Mn concentration (Fig. 1B), we assumed that the high fluorescence species might include two Mn^{2+} ions.

4. Discussion

ATPase activity measurements with 3 mM ATP at pH 7.2, both in the absence (Fig. 1) and in the presence (Fig. 2A) of the calcium ionophore A23187, show a biphasic metal activation profile, indicating that two Mg^{2+} or two Mn^{2+}, with different affinities, are involved in maximal enzyme turnover. For maximal activity both millimolar Me and ATP are required. A second Me·ATP pair accelerates ATP hydrolysis with lower affinity. Figs. 1 and 2 show that there was no turnover activation by millimolar ATP without accompanying millimolar Me. Moreover, high free ATP had an inhibitory effect on ATPase activity (Figs. 1 and 2B). It was previously observed that high free ATP (not Mg·ATP) in dephosphorylation media accelerates dephosphorylation (a rate-limiting step in enzyme cycling) [25]. However, since the ATPase had been previously phosphorylated with Pi in the presence of 20 mM $MgCl_2$, the two Mg^{2+} could already be bound to the cationic sites. On the other hand, Me concentrations higher than those required for maximal activation inhibited enzyme cycling. High concentrations of metal are clearly observed as inhibitory for ATPase activity. The main reason for such observation seems a modulation of calcium binding rather than participation of metal as cofactor with ATP [1].

We took advantage of acidic pH to investigate Mn and ATP binding without enzyme cycling and ATP hydrolysis. High-affinity Mn binding was measured using [^{54}Mn]Mn (Fig. 4) and ATP binding was evaluated through the ATP-dependent variation in ATPase intrinsic fluorescence (Fig. 5). We looked for a binding model for ATP and Mn^{2+} to explain these results (Scheme 2). ATP and Mn^{2+} bound to the enzyme one in the absence of the other (Figs. 4 and 5A). Fig. 4 shows that ATP up to 0.03 mM increased Mn^{2+} affinity and Fig. 5B shows that Mn^{2+} increased ATP affinity. Therefore, we put forward a random binding model (Scheme 2, Model 1; K_i (M) are dissociation constants), where the sequential binding of the ligands exhibits positive cooperativity as previously proposed by Reinstein and Jencks for Mg^{2+} and ATP [32]. The formation of Mn·ATP from Mn and ATP was considered. The apparent dissociation constant for Mn·ATP at pH 5.5 (K_1) was calculated from Goldstein absolute constants [28]. As measurements were made in the absence of Ca enough to bind to the transport sites, E represents the E_2 conformation of the ATPase.

K_3 and K_5 were as given above for the binding of each ligand with the enzyme, in the absence of the other. It follows that $K_3 \cdot K_4$ must be equal to $K_5 \cdot K_6$; thus, K_5 and K_3 were divided by a factor of 2–3 to obtain K_4 and K_6, respectively, to account for the increased Mn affinity upon [ATP] increase up to 30 μM and the increased ATP affinity in the presence of 0.1 mM $MnCl_2$. The final product (E·Mn·ATP) is independent of the order of addition of ATP and Mn^{2+}, since the fluorescence change is similar whatever the order of addition of the ligands.

However, model 1 was incomplete to explain millimolar Mn effect on ATP binding (Fig. 5B). As both 0.1 and 5 mM Mn are high enough to form E·Mn·ATP (K_6=6–9 μM), simulation of $\Delta F/F$% as function of free [ATP] according this simple model gives a unique curve for both [$MnCl_2$] (dotted line in Fig. 5B). To explain why the two experimental curves in Fig. 5B are not superposed, we included the intermediate $E{\cdot}Mn_2$ (Model 2), as in our model for the phosphorylation of the enzyme with Pi [20]. Full lines in Fig. 5B were obtained simulating the model 2, assigning the following fluorescence levels: 3.2% to E·ATP, 2.9% to E·Mn·ATP and 4.3% to $E{\cdot}Mn_2{\cdot}$ATP. High affinity ATP binding to EMn_2 (K_9) could explain why 5 mM $MnCl_2$ had an

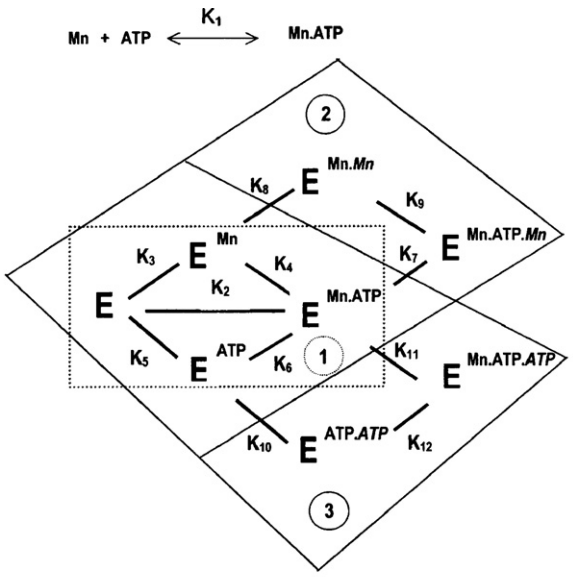

$K_1 = 3.3\ 10^{-4}$, $K_2 = 1.1\text{-}3.3\ 10^{-7}$, $K_3 = 1.8\ 10^{-5}$, $K_4 = 2.0\text{-}6.0\ 10^{-6}$, $K_5 = 0.6\text{-}1.2\ 10^{-5}$, $K_6 = 6.0\text{-}9.0\ 10^{-6}$, $K_7 = 5.0\ 10^{-4}$, $K_8 = 3.0\ 10^{-3}$, $K_9 = 1.0\ 10^{-6}$, $K_{10} = 6.0\ 10^{-6}$, $K_{11} = 6.0\ 10^{-4}$, $K_{12} = 6.0\ 10^{-5}$

Scheme 2.

additional positive effect on ATP binding with respect to 0.1 mM $MnCl_2$. The existence of a different ternary complex that requires higher Mn concentration to be formed ($E{\cdot}Mn_2{\cdot}$ATP) justifies the higher fluorescence increment reached in the presence of 5 mM $MnCl_2$ and enough ATP. Thus, ATP binding is favored if 2 Mn^{2+} are already bound to the enzyme ($K_9 < K_4$). The existence of a second metal site is also supported by ATPase activation at millimolar ATP and Me^{2+} (Figs. 1 and 2), and by Mn^{2+} stoichiometry in ATPase phosphorylation with Pi [20]. The introduction of two Me^{2+} ions to explain the above-discussed results agree with the structures of the SR Ca–ATPase recently reported from crystals formed in the presence of ADP and phosphate analogue [24,33]. The structures show two Mg^{2+} ions located in the vicinity of the catalytic site, one close to the phosphorylation site (D351) and a second link to the ADP. The authors concluded that both cations participate in the reaction of phosphorylation of the enzyme by ATP.

Model 1 was neither enough to adjust Mn binding data. According this simple model, the only way to explain the inhibition in Mn binding observed at ATP concentrations higher than 0.03 mM is by free Mn^{2+} decrease. Being free ATP higher than free Mn^{2+}, the Mn-deprived intermediate (E·ATP) would be the predominant species, diminishing those ones binding Mn (E·Mn and E·Mn·ATP). The model fitted in with the experimental values below 30 μM ATP (Mn binding was favored by previous ATP binding ($K_6 < K_3$)) but was not enough to justify the observed larger inhibition at higher [ATP] (dotted line in Fig. 4, inset). To explain the inhibition caused by ATP on Mn^{2+} binding–much stronger than predicted by Model 1 even if K_1 were arbitrarily diminished–we had to include in the model the binding of a second ATP with $K_d < 0.1$ mM, having $E{\cdot}ATP_2$ much lower affinity for Mn^{2+} than E·ATP (K_{12} vs. K_6 in Scheme 2, Model 3), as if high affinity metal locus were covered by ATP molecules. Although a second ATP site with such affinity was no reported, our fluorescence measurements shown in Fig. 5A might be fitted with two K_d around 6 and 60 μM. The full line in the inset of Fig. 4 was obtained with the 2 ATP–low Mn model (Model 3) and fitted in with Mn binding results. Other experimental data may support such hypothesis: (i) ATP dependence of [^{14}C]ATP binding in the absence of Ca^{2+} and Mg^{2+} was pH-independent [3] and the Scatchard plot gave a K_d of 20 μM for a stoichiometry of 3.5 nmol bound ATP per mg of protein, which corresponds to 1 ATP/ATPase molecule. However, 2 ATP sites, with K_d 11 μM and 80 μM and maximum bindings of 3 and 6 nmol ATP/mg protein, could also be deduced from the Scatchard plot of the same data. This alternative interpretation of [^{14}C]ATP binding data cannot be discarded and may support the hypothesis of two different ATP sites in the cation-free enzyme with K_d of 6–11 μM and 60–80 μM. (ii) Recent structural data [33] show that one nucleotide could be observed far away (14 Å) from phosphorylation site. We may speculate that different spatial arrangement of the cytoplasmic domains could fit two nucleotides, one close to the phosphorylation site and the other further apart within the structure. (iii) Other recent structural data [34] may also suggest the possible presence of two nucleotides within the same structure. Indeed, the covalently phosphorylated FITC labeled Ca–ATPase has its nucleotide site occupied by FITC, but also shows a high density corresponding to decavanadate between its N and A domains [35]. Size of decavanadate is compatible with an ATP molecule and it might be interpreted that two different nucleotide sites are revealed in this structure. This second bound ATP molecule might replace ADP after its departure, becoming hydrolysed in the next cycle.

From a functional point of view, the reduced ATPase activity observed with 3 mM ATP at low Me^{2+} concentrations (Figs. 1 and 2) is in accordance with the strong inhibitory effect of ATP >0.03 mM on [^{54}Mn]Mn binding (Fig. 4). When [ATP] is higher than [Mn], free [Mn] is reduced and the non-phosphorylatable species (E·ATP and E·ATP_2) accumulate as "non-transporting species". Conversely, in the presence of high metal concentration, millimolar ATP concentrations activate the enzyme cycling and, accordingly, a second ATP site with K_d 0.3–0.5 mM was reported when experiments were done in the presence of 5 mM $MgCl_2$ [10,11], values which are in accordance with K_{11} in Model 2.

High affinity Mn binding at pH 7.2 in the absence of calcium chelators (Fig. 3) showed little difference with results obtained at pH 5.5 (Fig. 4), indicating that E_1·Ca_2 and E_2 have similar affinity for the metal cosubstrate. Competition between Mn and Mg for the high affinity metal site at pH 7.2 showed a K_d for Mg^{2+} around 0.9 mM (Fig. 3). This value is in accordance with the reported Mg^{2+} affinity for the catalytic site in E_1·Ca_2 (K_d=0.94 mM) [32], measured through Mg^{2+} participation in enzyme phosphorylation by ATP at pH 7.2. On the contrary, other determinations of Mg binding gave higher K_d values but instead of being related with ATP-dependent phosphorylation they would be involved in modulation of calcium binding [1]: Guillain et al. found a K_d of 5 mM measuring intrinsic fluorescence changes induced by Mg^{2+} [36], and Schwartz and Inesi obtained a K_d of 7 mM with calorimetric measurements at pH 7 [7]. Although our K_d for Mg binding was 100–200 times higher than K_d for Mn (Fig. 3), K_m for Mn (≅10 μM) was only 10 times higher than K_m for Mg (≅100 μM) when ATPase activity was measured with 30 μM ATP (Fig. 1). The difference could be explained by the different positive effect of ATP on Mg^{2+} and Mn^{2+} binding; Reinstein and Jencks deduced that the interaction with bound ATP increases the affinity of the enzyme for Mg^{2+} by ~100-fold [32], and we showed an affinity increment of only ~3-fold for Mn^{2+} (K_6 vs. K_3 in the models).

In conclusion, the measured binding of ATP and Mn is well described by models including two ATP and one Mn (low Mn-model for ^{54}Mn binding data) or two Mn and one ATP (high Mn-model for fluorescence data). Depending on the ligand concentrations, the equilibrium is reached mainly according to model 1, 2 or 3. The ATPase activity determinations suggest the participation of two ATP molecules and two metal cofactor ions in the enzyme cycle. We show the well known activation by millimolar ATP, together with others not so well studied phenomena: (i) a complex dependence of the ATPase activity upon increasing the Me^{2+} concentrations at high [ATP], and (ii) an inhibitory effect of high ATP concentrations at low [Me^{2+}]. The Me and ATP interacting sites described here are compatible with recent reports of structural data and with the observed characteristics of the ATPase activity.

Acknowledgments

This work was supported by grants from the "Universidad de Buenos Aires" and the "Consejo Nacional de Investigaciones Científicas y Técnicas and The Centre national de la Recherche Scientifique".

References

[1] V. Forge, E. Mintz, F. Guillain, Ca^{2+} binding to sarcoplasmic reticulum ATPase revisited: I. Mechanism of affinity and cooperativity modulation by H^+ and Mg^{2+}, J. Biol. Chem. 268 (1993) 10953–10960.
[2] C. Peinelt, H.J. Apell, Kinetics of the Ca(2+), H(+) and Mg(2+) interaction with the ion-binding sites of the SR Ca–ATPase, Biophys. J. 82 (2002) 170–181.
[3] J.J. Lacapère, N. Bennett, Y. Dupont, F. Guillain, pH and magnesium dependence of ATP binding to sarcoplasmic reticulum ATPase, J. Biol. Chem. 265 (1990) 348–353.
[4] H.R. Kalbitzer, D. Stehlic, W. Hasselbach, The binding of calcium and magnesium to sarcoplasmic reticulum vesicles as studied by manganese electron paramagnetic resonance, Eur. J. Biochem. 82 (1978) 245–255.
[5] S. Yamada, N. Ikemoto, Reaction mechanism of calcium ATPase of sarcoplasmic reticulum. Substrates for phosphorylation reaction and back reaction, and further resolution of phosphorylated intermediates, J. Biol. Chem. 255 (1980) 3108–3119.
[6] Y. Takakuwa, T. Kanazawa, Reaction mechanism of (Ca^{2+}, Mg^{2+})–ATPase of sarcoplasmic reticulum. The role of Mg^{2+} that activates hydrolysis of the phosphoenzyme, J. Biol. Chem. 257 (1982) 426–431.
[7] F.P. Schwartz, G. Inesi, Entropic drive in the sarcoplasmic reticulum ATPase interaction with Mg^{2+} and Pi, Biophys. J. 73 (1997) 2179–2182.
[8] S. Wakabayashi, M. Shigekawa, Effect of metal bound to the substrate site on calcium release from the phosphoenzyme intermediate of sarcoplasmic reticulum ATPase, J. Biol. Chem. 262 (1987) 11524–11531.
[9] T. Ogurusu, S. Wakabayashi, M. Shigekawa, Activation of sarcoplasmic reticulum Ca^{2+}–ATPase by Mn^{2+}: an Mn^{2+} binding study, J. Biochem. 109 (1991) 472–476.
[10] Y. Dupont, Kinetics and regulation of sarcoplasmic reticulum ATPase, Eur. J. Biochem. 72 (1977) 185–190.
[11] P.C. Carvalho-Alves, C.R.G. Oliveira, S. Verjovski-Almeida, Stoichiometric photolabeling of two distinct low and high affinity nucleotide sites in sarcoplasmic reticulum ATPase, J. Biol. Chem. 260 (1985) 4282–4287.
[12] R.J. Coll, A.J. Murphy, Sarcoplasmic reticulum CaATPase: product inhibition suggests an allosteric site for ATP activation, FEBS Lett. 187 (1985) 131–134.
[13] R.J. Coll, A.J. Murphy, Kinetic evidence for two nucleotide binding sites on the Ca–ATPase of sarcoplasmic reticulum, Biochemistry 30 (1991) 1456–1461.
[14] J.E. Bishop, M.K. Al-Shawi, G. Inesi, Relationship of the regulatory nucleotide site to the catalytic site of the sarcoplasmic reticulum Ca^{2+}–ATPase, J. Biol. Chem. 262 (1987) , 4658–4663.
[15] J.J. Lacapère, F. Guillain, The reaction mechanism of Ca^{2+}–ATPase of sarcoplasmic reticulum. Direct measurement of the Mg·ATP dissociation constant gives similar values in the presence or absence of calcium, Eur. J. Biochem. 211 (1993) 117–126.
[16] J.D. Clausen, D.B. McIntosh, B. Vilsen, D.G. Woolley, J.P. Andersen, Importance of conserved N-domain residues Thr441, Glu442, Lys515, Arg560, and Leu562 of sarcoplasmic reticulum Ca^{2+}–ATPase for MgATP binding and subsequent catalytic steps. Plasticity of the nucleotide-binding site, J. Biol. Chem. 30 (2003) 20245–20258.
[17] P.J. Garrahan, A.F. Rega, G.L. Alonso, The interaction of magnesium ions with the calcium pump of sarcoplasmic reticulum, Biochim. Biophys. Acta 448 (1976) 121–132.
[18] T. Ogurusu, S. Wakabayashi, M. Shigekawa, Functional characterization of lanthanide binding sites in the sarcoplasmic reticulum Ca^{2+}–ATPase: do lanthanide ions bind to the calcium transport site? Biochemistry 30 (1991) 9966–9973.
[19] E. Mintz, J.-J. Lacapére, F. Guillain, Reversal of the sarcoplasmic reticulum ATPase cycle by substituting various cations for magnesium. Phosphorylation and ATP synthesis when Ca^{2+} replaces Mg^{2+}, J. Biol. Chem. 265 (1990) 18762–18768.
[20] D.A. González, G.L. Alonso, J.J. Lacapère, Manganese as a cosubstrate for the phosphorylation of the sarcoplasmic reticulum Ca-dependent adenosine triphosphatase with orthophosphate, Biochim. Biophys. Acta 1276 (1996) 188–194.

[21] G. Patchornik, R. Goldshleger, S.J.D. Karlish, The complex ATP–Fe^{2+} serves as a specific affinity cleavage reagent in ATP–Mg^{2+} sites of Na,K–ATPase: altered ligation of Fe^{2+} (Mg^{2+}) ions accompanies the $E_1P \rightarrow E_2P$ conformational change, Proc. Natl. Acad. Sci. U. S. A. 97 (2000) 11954–11959.

[22] J.M. Shin, R. Goldshleger, K.B. Munson, G. Sachs, S.J.D. Karlish, Selective Fe^{2+}-catalyzed oxidative cleavage of gastric H^+,K^+–ATPase: implications for the energy transduction mechanism of P-type cation pumps, J. Biol. Chem. 276 (2001) 48440–48450.

[23] S. Hua, G. Inesi, H. Nomura, C. Toyoshima, Fe^{2+}-catalyzed oxidation and cleavage of sarcoplasmic reticulum ATPase reveals Mg^{2+} and Mg^{2+}–ATP sites, Biochemistry 41 (2002) 11405–11410.

[24] T.L.-M. Sorensen, J.V. Moller, P. Nissen, Phosphoryl transfer and calcium ion occlusion in the calcium pump, Science 304 (2004) 1672–1675.

[25] P. Champeil, F. Guillain, Rapid filtration study of the phosphorylation-dependent dissociation of calcium from transport sites of purified sarcoplasmic reticulum ATPase and ATP modulation of the catalytic cycle, Biochemistry 25 (1986) 7623–7633.

[26] O.H. Lowry, N.J. Rosebrough, A.L. Farr, N.J. Randall, Protein measurement with the Folin phenol reagent, J. Biol. Chem. 193 (1951) 265–275.

[27] E.S. Baginski, P.P. Foa, B. Zak, Determination of phosphate: study of labile organic phosphate interference, Clin. Chim. Acta 15 (1967) 155–158.

[28] D.A. Goldstein, Calculation of the concentrations of free cations and cation–ligand complexes in solutions containing multiple divalent cations and ligands, Biophys. J. 26 (1979) 235–242.

[29] M. Chiesi, G. Inesi, Adenosine 5′-triphosphate fluxes of manganese and hydrogen ions in sarcoplasmic reticulum vesicles, Biochemistry 19 (1980) 2912–2918.

[30] D.A. González, M.A. Ostuni, J.-J. Lacapère, G.L. Alonso, A model accounting for the simultaneous transport of calcium and manganese in sarcoplasmic reticulum membranes, Ann. N.Y. Acad. Sci. 986 (2003) 320–322.

[31] Y. Dupont, F. Guillain, J.J. Lacapère, Fluorimetric detection and significance of conformational changes in Ca^{2+}–ATPase, Methods Enzymol. 157 (1988) 206–219.

[32] J. Reinstein, W.P. Jencks, The binding of ATP and Mg^{2+} to the calcium adenosinetriphosphatase of sarcoplasmic reticulum follows a random mechanism, Biochemistry 32 (1993) 6632–6642.

[33] C. Toyoshima, H. Nomura, T. Tsuda, Lumenal gating mechanism revealed in calcium pump crystal structures with phosphate analogues, Nature 432 (2004) 361–368.

[34] D.L. Stokes, F. Delavoie, W.J. Rice, P. Champeil, D. McIntosh, J.-J. Lacapère, Structural studies of a stabilized phosphoenzyme intermediate, J. Biol. Chem. 280 (2005) 18063–18072.

[35] E. Beaumont, B. Fournier, D. Stokes, K. Hinsen, J.-J. Lacapère, Atomic structure of a covalently phosphorylated intermediate of SERCA1 Ca^{2+}–ATPase: normal mode fits of electron densities, J. Gen. Physiol. 126 (2005) 13a.

[36] F. Guillain, M.P. Gingold, P. Champeil, Direct fluorescence measurements of Mg^{2+} binding to sarcoplasmic reticulum ATPase, J. Biol. Chem. 257 (1982) 7366–7371.